

Interactions of molten salts with cathode products in the FFC Cambridge Process

(Authorship: see the Title page)

Abstract

Molten salts play multiple important roles in the electrolysis of solid metal compounds, particularly oxides and sulfides, for extraction of metals or alloys. Some of these roles are positive in assisting the extraction of metals, such as dissolving the oxide or sulfide anions, and transporting them to the anode for discharging, and offering the high temperature to lower the kinetic barrier to break the metal-oxygen or metal-sulfur bond. However, there are also unfavourable effects, including electronic conduction and significant capability of dissolving oxygen and carbon dioxide gases. In addition, although molten salts are relatively simple in terms of composition, physical properties and decomposition reactions at inert electrodes, in comparison with aqueous electrolytes, the high temperatures of molten salts may promote unwanted electrode-electrolyte interactions. This article reviews briefly and selectively research and development of the FFC Cambridge Process in the past two decades, focusing on observations, understanding and solutions of various interactions between the molten salts and the cathodes at different reduction states, including perovskitisation, non-wetting of molten salts on metals, carbon contamination to products, formation of oxychlorides and calcium intermetallic compounds, and oxygen transfer from air to the cathode product mediated by oxide anions in the molten salt.

Keywords: FFC Cambridge Process, molten salts, electrolysis, extraction, oxides, sulfides, metals, alloys, reaction mechanisms

1. Background

In December 1999, the University of Cambridge published an international patent on what is now known widely as the Fray-Farthing-Chen (FFC) Cambridge Process. It is about electrolytic extraction of metals and alloys directly from their solid compounds in molten salts [1]. Preliminary findings from testing the FFC Cambridge Process were soon reported in a

Letter to Nature for the extraction of titanium from titanium dioxide (TiO_2) in molten calcium chloride (CaCl_2) [2]. The report aroused enthusiastic responses, both positive and critical, from global communities of titanium technologists and researchers [3-5]. In the past two decades, world-wide research and development have confirmed the scientific principle and technical feasibility and flexibility of the process for the extraction of almost all metals listed in the periodic table and their alloys from the respective oxide or sulfide precursors [6-14]. In addition, the FFC Cambridge Process has been shown to have versatile applications in other fundamental and industrial areas such as near-net shape manufacturing of metallic artefacts of complex structures, medical implants, oxygen generation on the Moon, capture and electrolytic conversion of carbon dioxide CO_2 to various forms of solid carbon, e.g. carbon nanotubes, carbon monoxide (CO) and hydrocarbon fuels ($\text{C}_n\text{H}_{2n+2}$, $n < 10$), and rechargeable molten salt metal-air batteries [15-22].

2. Basic electrochemistry

The main claim of the FFC Cambridge Process is very general and states a method “for removing a substance (X) from a solid metal, a metal compound or semi-metal compound (M^1X) by electrolysis in a fused salt of M^2Y or mixture of salts, which comprises conducting the electrolysis under conditions such that reaction of X rather than M^2 deposition occurs at an electrode surface, and that X dissolves in the electrolyte M^2Y .” This claim makes it very clear that the cathode can be a metal containing another substance (e.g. impurity) or a metal or semi-metal compound, including but not limited to metal oxides which have been mostly studied in the past two decades. It is interesting to point out that later research has demonstrated that the electrolysis of metal sulfides is actually quicker and more efficient than that of metal oxides, but the invention of FFC Cambridge Process was mostly based on the initial study of electrochemical reduction of TiO_2 to Ti metal in molten CaCl_2 , which is now known as one of the few most difficult metal oxides to electrolyse.

In terms of thermodynamics [23], electrolysis of TiO_2 should be fairly feasible, following Reaction (1) or (2) and (3) on an inert or carbon anode, respectively. Note that

although Reaction (3) seems more feasible than Reaction (2) on a carbon anode, the highly spontaneous Reaction (4) makes CO₂ effectively the main product on the carbon anode. This view can be further explained. With $\log K = 2\log p_{\text{CO}_2} - (2\log p_{\text{CO}} + \log p_{\text{O}_2}) = 16.1$, it can be established that $p_{\text{CO}_2} \gg (p_{\text{CO}} + p_{\text{O}_2})$ and $(p_{\text{CO}_2} + p_{\text{CO}} + p_{\text{O}_2}) \approx 1$ atm for bubbles of the mixed anode gases to escape from the anode surface. Therefore, $\log (p_{\text{CO}}/p_{\text{O}_2}) = - (16.1 + \log p_{\text{CO}}) \approx -16$, which indicates the amount of CO to be negligible in comparison with that of O₂ formed on the carbon anode. Of course, the validity of thermodynamic predictions can be affected by the electrode kinetics, whilst experimental studies have confirmed the anodic formation of O₂ on carbon in molten CaCl₂ [20,24,25]



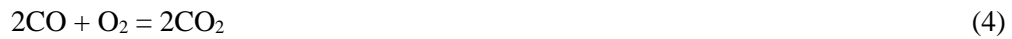
$$\Delta G^\circ (900 \text{ }^\circ\text{C}) = 732.1 \text{ kJ}; \quad \Delta E^\circ = 1.897 \text{ V (inert anode)}$$



$$\Delta G^\circ (900 \text{ }^\circ\text{C}) = 336.1 \text{ kJ}; \quad \Delta E^\circ = 0.871 \text{ V (carbon anode)}$$

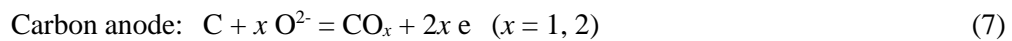


$$\Delta G^\circ (900 \text{ }^\circ\text{C}) = 300.7 \text{ kJ}; \quad \Delta E^\circ = 0.779 \text{ V (carbon anode)}$$



$$\Delta G^\circ (900 \text{ }^\circ\text{C}) = -360.6 \text{ kJ}; \quad \log K = 16.1$$

Reactions (1) to (3) are possible cell reactions, whilst electrode reactions are as follows.



Reaction (5) represents electrochemical reduction, or deoxidation of TiO₂. The same can be written for other metal oxides. Thus, electro-deoxidation and electro-reduction are both used in the literature as the scientific terms in place of the FFC Cambridge Process.

Figure 1a illustrates schematically a typical laboratory molten salt electrolysis cell for studying the FFC Cambridge Process. This two electrode cell is suitable for electro-reduction of metal oxides and other compounds at the gram scale. Note that the lower part of the steel

vessel (or retort) extrudes below and outside the furnace so that it remains at temperatures much lower than that of the molten salt. In this way, any molten salt dripping or condensing at the welding joint between the wall and bottom of the retort will solidify and become non-corrosive [18]. It can also be readily modified into a three electrode cell for fundamental analyses by, for example, cyclic voltammetry and chronoamperometry.

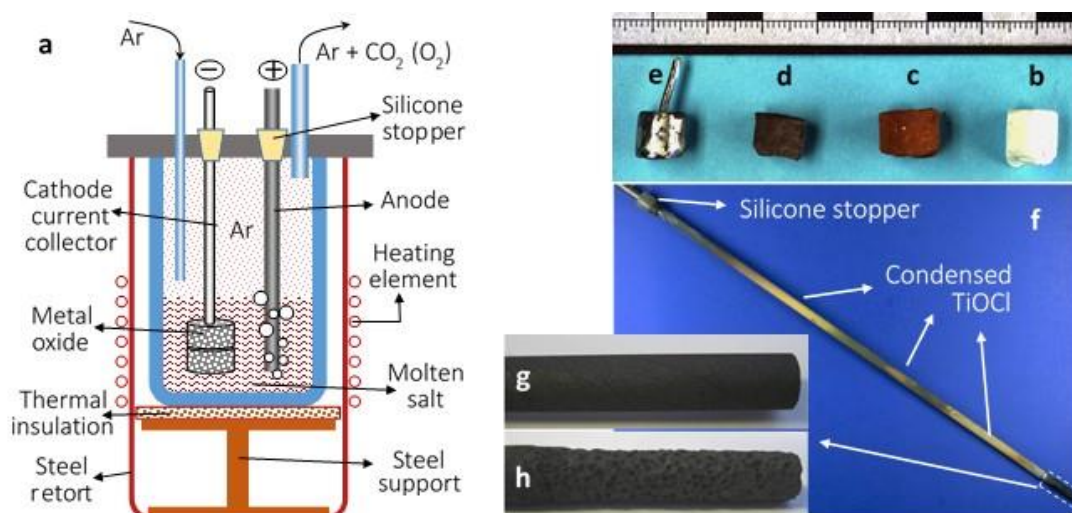


Figure 1. (a) Schematic diagram of a molten salt electrolyser for laboratory study of the FFC Cambridge Process. The external diameter of the steel retort is typically 15 cm. (b - h) Digital photographs of slip-cast and sintered pellets of TiO_2 (b), mixed TiO_2 , Al_2O_3 and V_2O_5 (c), electro-reduced c (d), surface polished d (e), and a long graphite rod (ca. 1.6 cm in diameter) anode after electrolysis of TiO_2 (f), the lower end of the graphite rod before (g) and after 24 hr electrolysis (h).

Electrode materials selection is crucial to ensure the success of the FFC Cambridge Process. For the cathode, Figure 1b and 1c show the pellets of TiO_2 (white) and mixed TiO_2 , Al_2O_3 and V_2O_5 (brown) that were to attach to, and be electro-reduced on the cathode current collector. The products in Figure 1d and 1e were the Ti-6Al-4V alloy before and after light polishing. For the anode, because of their easy availability, ease of shaping and low cost, commercial graphite products, particular rods (see Figure 1f) and plates, have been commonly used to make the anode or counter electrode in various studies on the FFC Cambridge

Process, although quality of commercial graphite varies significantly. Poor quality graphite may suffer from the attack of oxidation and gas bubbling, leading to graphite erosion as shown clearly by comparison between Figure 1g and 1h, and unwanted carbon debris off the anode. The carbon debris can float on, or suspend in the molten salts, causing electronic conduction to lower electrolysis efficiency and contamination of the product on the cathode. More discussions are given later on the issues from using a graphite anode. Glassy carbon can also be used to make the anode or working electrode in studies of molten salts, particularly for fundamental analysis by cyclic voltammetry [26,27]. Like graphite, glassy carbon also suffers from electrochemical oxidation in presence of oxide ions, and hence is too expensive to use in bulk electrolysis.

In addition, it has been recognised that the discharge (electro-oxidation) of oxide ions (O^{2-}) on a carbon electrode suffers from serious kinetic difficulties [26,27]. These complex kinetic steps lead to a fast increase of polarisation with increasing the current density on the anode. The kinetics are partly responsible for the practically applied cell voltage for electrolysis of TiO_2 to be at or greater than 3.00 V, in contrast to the thermodynamic predictions of around 1.00 V according to Reactions (2) and (3). To minimise such kinetic barriers, the surface area of the graphite anode in contact with the molten salt should be as large as realistically possible. It was found that the anodic polarisation could be reduced by about 1.0 V when the graphite anode surface area was increased by 10 times [27].

Alternatively, inert anodes should be considered as an option.

By definition, inert anodes should be inactive and non-consumable, and would work without all the problems resulting from using carbon. Although the potential for anodic formation of O_2 is about 1.00 V higher than that for CO_2 formation, see Reactions (1) and (2), this benefit of using carbon anodes could be largely lost to the above mentioned kinetic polarisation. There are two types of ceramic based inert anode: ion blocking and ion conducting as explained in Figure 2a and 2b, respectively. Several materials have been tested for making ion blocking inert anodes, including tin oxide (SnO_2) with or without copper doping, and calcium ruthenate ($CaRuO_3$) with or without titanium substitution [28,29].

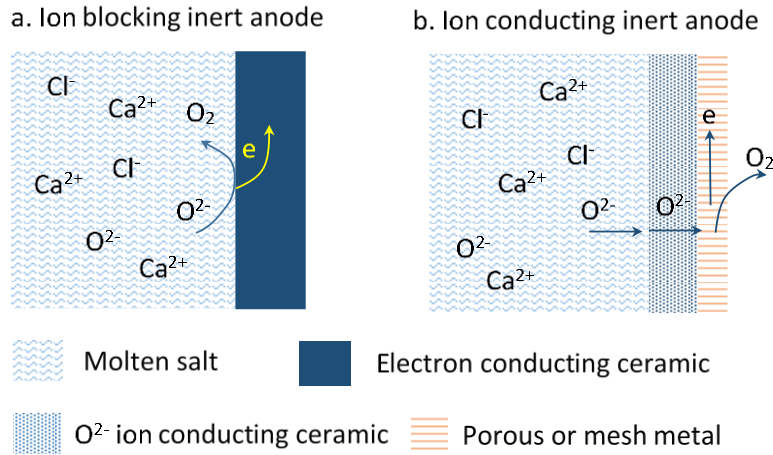


Figure 2. Schematic illustrations of the working mechanisms of the (a) ion blocking inert anode and (b) ion conducting inert anode.

Ion conducting inert anodes are constructed with a membrane of oxide ion conductor, typically yttria stabilized zirconia (YSZ) in the form a tube with a closed end. One side of the membrane, the wet side, faces the molten salt to connect O²⁻ conduction into the membrane. The other side, or dry side of the membrane can be made in contact with a liquid or solid metal, e.g. tin (Sn) or silver (Ag), with relatively high diffusivity and solubility of atomic oxygen [30,31]. Oxidation of O²⁻ ions occurs at the YSZ/ metal interface with the produced atomic oxygen dissolving in, and diffusing through the metal to the metal/air interface where the O₂ gas forms and escapes. Alternatively, the dry side of the YSZ membrane may be coated with a porous platinum (Pt) paste in which is buried a Pt mesh or wires as the current collector. Oxidation of O²⁻ is catalysed by Pt at the YSZ/Pt/air three phase interlines (3PIs) with the produced O₂ gas escaping through the pores in the paste into air [32]. The main issues of ceramic based anodes include their highly temperature dependent resistivity, thermal cyclability and related costs.

It is worth mentioning that graphite anodes are almost fully inert for discharging sulfide ions (S²⁻) to the sulfur vapour (S₂) [33,34], and chloride ions (Cl⁻) to the chlorine gas (Cl₂) [35,36] in molten chlorides. In electrolytes with high oxide ion activity, such as molten

carbonates and mixed oxide melts, refractive metals with high tendency to form a stable surface oxide layer may also be used as ion blocking inert anodes [37-39]. However, a few metals, e.g. iridium (Ir) and silver (Ag) do not form stable oxides at high temperatures, and may behave sufficiently stable as an inert anode in some molten salts [12,40,41].

3. Perovskitisation of metal oxides on cathode

In a laboratory cell as shown in Figure 1a, the cell voltage applied for electrolysis of TiO₂ is usually about 3.00 V with a graphite anode, although the thermodynamic prediction from Reactions (2) and (3) is less than 1.00 V. Apart from the kinetic difficulties on a carbon anode as mentioned above, cathodic processes also contribute. First, it is partly related to the multiple intermediate phases between TiO₂ and the Ti metal. At the electrolysis temperature (850 to 950 °C), these phases include Ti_nO_{2n-1} (n ≥ 2, Magneli phase), Ti₂O₃, TiO, Ti_yO (y = 1.5 and 2, pseudo-oxides) and solid oxygen solution. Thus, it can be expected that the electro-reduction of TiO₂ will pass through each of these phases before reaching the final metallic phase. From available thermodynamic data [23], the cell voltages needed to decompose TiO and Ti₃O₂ with an inert or carbon anode are given below for Reactions (8) to (11). It is worth pointing out that when the oxygen activity is lower than that in TiO or Ti₃O₂, O and Ti combine into a solid solution from which oxygen removal becomes increasingly controlled by O diffusion in Ti with a secondary effect from the applied cathode potential.



$$\Delta G^\circ (900 \text{ }^\circ\text{C}) = 860.9 \text{ kJ}; \quad \Delta E^\circ = 2.231 \text{ V (inert anode)}$$



$$\Delta G^\circ (900 \text{ }^\circ\text{C}) = 863.5 \text{ kJ}; \quad \Delta E^\circ = 2.237 \text{ V (inert anode)}$$

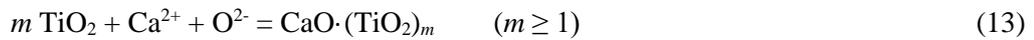
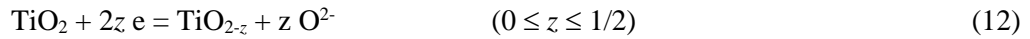


$$\Delta G^\circ (900 \text{ }^\circ\text{C}) = 464.9 \text{ kJ}; \quad \Delta E^\circ = 1.205 \text{ V (carbon anode)}$$

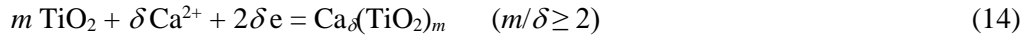


$$\Delta G^\circ (900 \text{ }^\circ\text{C}) = 467.4 \text{ kJ}; \quad \Delta E^\circ = 1.211 \text{ V (carbon anode)}$$

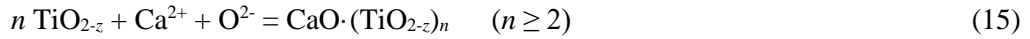
These are small changes compared with those of Reactions (1) and (2), and not enough to account for the experimental observation of 3.00 V. Therefore, kinetics must have played important roles that lead to cathodic polarisation. These were found to be caused largely by the formation of various perovskites on the cathode during electrolysis, resulting from interactions between original and partially reduced TiO_2 and the calcium dication (Ca^{2+}) [7,42,43]. Perovskitisation happens in both electrochemical and chemical ways as exemplified below. TiO and Ti_3O_2 seem to have no chemical interaction with Ca^{2+} ions.



($\text{CaO} \cdot (\text{TiO}_2)_m$ becomes CaTiO_3 at $m = 1$)



($\text{Ca}_\delta(\text{TiO}_2)_m$ becomes CaTi_2O_4 at $m/\delta = 2$)



($\text{CaO} \cdot (\text{TiO}_{2-z})_n$ becomes CaTi_2O_4 at $n = 2, z = 0.5$)

Reactions (13) to (15) add Ca^{2+} ions to the cathode oxide phase without any oxygen removal, leading to volume expansion of the solid phase, which in turn reduces or eliminates the pore volume in the cathode. As a result, pores for O^{2-} transport in the oxide cathode are partially or fully blocked, resulting in cathodic polarisation. In fact, perovskitisation also happens to the cathode of other metal oxides, such as chromium (Cr) and niobium (Nb) oxides [44,45].

There are two proposed and laboratory demonstrated approaches to avoid the impact of perovskitisation. The first approach uses ex situ perovskitisation, i.e. reacting TiO_2 with CaO or $\text{Ca}(\text{OH})_2$ at elevated temperatures (e.g. 1300 °C for 5 hrs) to form a porous CaTiO_3 precursor (cylindrical pellet) in air, and then using the CaTiO_3 precursor as the cathode for electrolysis in molten CaCl_2 . By doing so, perovskitisation will not occur to the CaTiO_3 cathode during electrolysis, but the cell voltage for electrolysis of CaTiO_3 should be slightly higher than that of TiO_2 as can be seen by comparing Reactions (16) and (2).



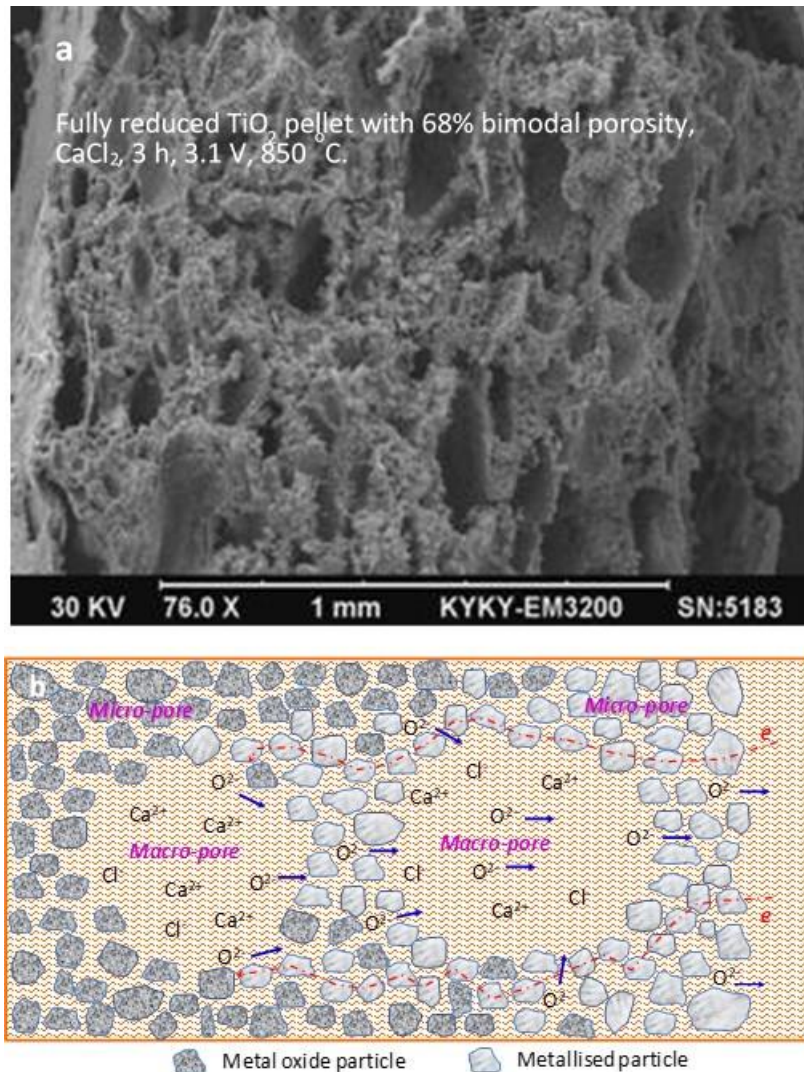
$$\Delta G^\circ (900 \text{ }^\circ\text{C}) = 423.7 \text{ kJ}; \quad \Delta E^\circ = 1.098 \text{ V (carbon anode)}$$

Initial tests of this approach were carried out at 3.20 V and 850 °C in molten CaCl₂ [43]. The results showed that under the same experimental conditions, electrolysis of CaTiO₃ was almost twice faster as electrolysis of TiO₂ to achieve Ti products of comparable purities. The higher speed of electrolysis was also a reflection of faster transportation of O²⁻ ions in the CaTiO₃ cathode than in the TiO₂ cathode. This is because electro-reduction of CaTiO₃ removes not only O²⁻ but also Ca²⁺ ions, leaving behind increased porosity. This is in contrast to electro-reduction of TiO₂ in which perovskitisation brings about increased volume of the solid phase and hence blockage of the pores in the oxide cathode, impeding removal of O²⁻ ions and the whole electrolysis. Note that continuous CaTiO₃ electrolysis via Reaction (16) will lead to accumulation of CaO in the molten salt. However, one can in principle combine Reactions (16) and (13) to form a closed loop in which CaO is cycled and functions like a “phase change catalyst” to accelerate the electrolysis of TiO₂.

The second approach is to simply increase the porosity of the TiO₂ cathode, using the low cost and recyclable NH₄HCO₃ as the fugitive porogenic agent. In most previous studies of the FFC Cambridge Process, the TiO₂ cathode had usually a porosity of 40 to 50 %. Because the molar volumes of TiO₂ and CaTiO₃ are 18.9 and 34.2 mL/mol, respectively, perovskitisation can lead to a volume increase up to 81 %. Obviously, when it happens inside the pores of the TiO₂ cathode of 40 to 50 % in porosity, partial blockage of the ion channels is inevitable. Because perovskitisation of the TiO₂ cathode proceeds with electro-reduction which follows the 3PI propagation mechanism [46-48], it is possible to bypass the effect of perovskitisation by increasing the TiO₂ cathode porosity to 60 to 80 % so that the formation rate of TiO and the pseudo-oxide phases surpasses the rate for perovskitisation. In other words, the perovskite phase, if formed, is unable to grow in size before further reduction.

This was indeed confirmed by experiments in which electro-reduction was found to be most effective when the porosity of the TiO₂ precursor was made about 68 % [49]. It was thought that at higher porosities, the cathode volume also increased, making the path and time

longer as well for O^{2-} ion to diffuse out of porous cathode. Another benefit was that the porous TiO_2 cathode prepared from using NH_4HCO_3 as the fugitive agent presented a micro-macro-bimodal porosity as shown in Figure 3a. It is understood that the macropores of over $100\ \mu m$ in length were left by the evaporation of the NH_4HCO_3 granules that were mixed, pressed and sintered together with the TiO_2 powder which alone would only form micropores



between the sub-micrometre particles. The sample shown in the SEM image in Figure 3a was fully metallised at 3.20 V in only 3 hrs, containing 6800 ppm O. Continuing the electrolysis at a lower voltage of 2.60 V for another 3 hrs led to a further decrease of the oxygen content to 1900 ppm, whilst the energy consumption was as low as 21.5 kWh/kg-Ti. This observation is evidence of a much smaller kinetic influence on removing oxygen from the metallised TiO₂ cathode.

Figure 3b further illustrates how the micro-macro-bimodal porous structure of the TiO₂ cathode benefits electro-reduction. Firstly, the cathodically produced O²⁻ may participate in either or both of two competing reactions: perovskitisation in the solid phase of the cathode, and dissolution into the liquid molten salt. Obviously, dissolution is beneficial to electro-reduction. Both reactions proceed with the assistance of Ca²⁺ ions whose activity in the molten salt can be assumed to be constant. Thus, the key to prevent perovskitisation, or keep it short-lived upon formation, is to maintain a low O²⁻ activity in the molten salt. This is very difficult, if not impossible, in the micropores that are present dominantly in the pressed and sintered pellets of TiO₂ powder of 40-50% in porosity.

With the use of NH₄HCO₃ to form the micro-macro-bimodal porous structure, the relatively large amount of molten salt in the macropores could help reduce the activity of O²⁻ ions below that is needed to precipitate CaO, preventing perovskitisation. Secondly, the transport of O²⁻ ions in the molten salt of the macropores should behave very much the same as in the bulk electrolyte with the diffusion coefficient in the range of 10⁻⁵ cm²/s, whilst in the micropores, the diffusion coefficient of O²⁻ is about 10⁻⁷ cm²/s. Therefore, with faster ion transportation and minimised effect of perovskitisation, it is not surprising that electro-reduction was much quicker in the micro-macro-bimodal porous TiO₂ cathode. Obviously, the proposed increase of 10 to 20% in cathode porosity may translate to reduced volumetric productivity, which should be well balanced by the benefits in both speed increase and energy saving from using a more porous cathode.

4. Non-wetting of molten salts on fully electro-reduced metals

It was found in the world's first 99.8 % pure Ti product from electro-reduction of TiO_2 in molten CaCl_2 that the porous oxide precursor turned into a porous metal, as shown in Figure 4a. A technical question asked then on the FFC Cambridge Process was how to remove the salt that had solidified inside the porous metallic products. Since CaCl_2 has a high solubility in water (100 g/mL) and most transition metals and their alloys are relatively stable in water, most, if not all, porous and powdery FFC metal samples reported in the literature were washed in water. Could it be fully effective to remove solidified salts hidden deep inside the pores? Also, because the nodular Ti particles were much larger than the spherical particles in the TiO_2 precursor, growth of the Ti particles must have happened. Therefore, would it be possible that in the course of Ti particle growth, molten CaCl_2 may be enclosed in the metal?

Analyses of the FFC Ti samples by SEM and XRD revealed interesting behaviour. As shown in Figure 4b, with careful selection and inspection, nanometre pores were found in the cross section of some relatively large but broken Ti nodules, but these were empty [50]. It could be argued that CaCl_2 were removed by washing the sample in water and drying before the SEM examination. However, such nanopores should also exist in many more unbroken Ti nodules. If these closed nanopores were filled with CaCl_2 , the salt should have been detected by XRD, but it was not [43,49]. A hypothesis had attributed the formation of nanopores to the space left after removal of the fairly large amount of oxygen in the initially formed metallic phases [50]. For example, the pseudo-oxide phase of Ti_3O_2 has an oxygen content of 18.2 wt%. This rationale is acceptable but it is not an account for the undetected CaCl_2 in the pores of the porous FFC Ti product.

Another explanation came to light when the cause for an incidental observation was considered. In an experiment for electro-deoxygenation of a Ti foil sample in a Ti crucible, both the foil and crucible were polarised negatively at -3.0 V against a common graphite anode. When electrolysis was near the designated time of completion, the Ti foil was moved forward and backward to drive away a thin layer of floating carbon debris. The manual operation incidentally led to the contact between the foil and crucible. What happened next

was surprisingly unexpected. The Ti foil was stuck to the Ti crucible, and the two were only separated after cooling and washing away the solidified salt, and forcing a screwdriver between the two with a hammer. Obviously, the Ti foil was welded to the Ti crucible. It is known that in the absence of impurities, such as oxide, pure metal to metal mixing occurs, resulting in an integral bond. This principle is the foundation of an industrial technique called friction welding. Although the friction generates heat and hence high temperatures to promote atom mobility during friction welding, the metals are still solid without melting [51]. In the case of Ti foil and Ti crucible, because both were negatively polarised for a sufficiently long time, their surfaces must have become oxygen-free and hence were able to weld or bond. However, there was the molten salt between the two Ti surfaces and why the welding still proceeded could only be explained by the molten salt being non-wetting to pure Ti surfaces.

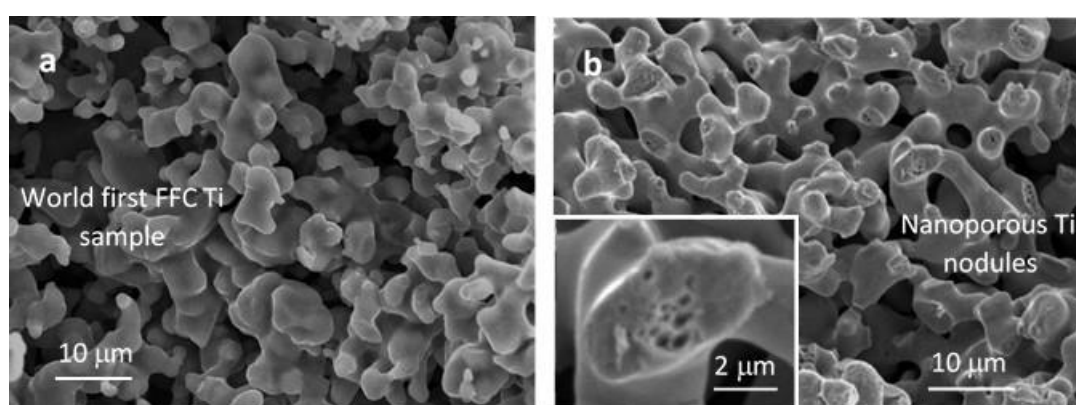


Figure 4. SEM images of (a) the first sample of FFC Ti of 99.7 % purity (EDX) produced in Cambridge in late 1997 with a porous structure formed by interconnected nodules of micrometres, and (b) FFC Ti nodules of which a few were broken, revealing nanometre pores as shown in the inset [50].

This understanding of non-wetting of molten salts on a pure metal surface accounts well for another observation of the absence or very little of salt being present in a well electro-reduced and very lightly washed pellet of mixed nickel, manganese and gallium oxide powders [52]. Later, purposely designed experiments studied the wetting of molten CaCl_2 on

the surface of terbium (Tb) metal [53]. In the first test, a fully electro-reduced (metallised) porous pellet of Tb_2O_3 (converted from Tb_4O_7) powder was cooled to room temperature and broken, without washing, into two halves to reveal the cross section which was directly analysed by SEM and EDX. As expected, $CaCl_2$ was only detected in the surface region (labelled A), whilst the contents of both Cl and Ca decreased quickly into the metallised pellet (from B to E) as shown in Figure 5a. The SEM image of nodules in Figure 5b was taken from the sand-paper ground surface of the fully metallised sample after rinsing in dimethyl sulfoxide (DMSO) to remove debris from grinding. It can be seen that these nodules were very clean, whilst $CaCl_2$ is insoluble in dry DMSO.

In the other experiment, a small sheet of pure Tb metal was drilled with 6 small holes of 1 mm in diameter, and immersed into molten $CaCl_2$ in air. Upon removing the Tb sample from the molten salt, cooled in air, and scraping away the skin of solidified salt, it was seen that all the 6 holes were filled with solidified salt. This change, as presented in Figure 5c and 5d, is understandable because the Tb metal surface was covered with a thin oxide layer on which the molten salt could wet. The Tb sheet was then placed back into the molten salt, electro-reduced against a graphite anode at 3.2 V for 30 min under argon. After electrolysis, the electro-reduced Tb sheet was removed from the molten salt and cooled in air. It was then seen that 5 of the 6 holes were empty. These empty holes must have resulted from the electro-reduced Tb sheet surface being free of oxygen. As a result, the walls of the small holes were unwettable by the molten salt which was driven out of the holes by gravity when the Tb sheet was lifted above the molten salt.

In conclusion, past experimental observations have proven qualitatively but conclusively that molten $CaCl_2$ does not wet the wall surfaces of the internal pores in fully electro-metallised metal oxides cathodes. This finding is theoretically accountable, and practically meaningful to the engineering design of the FFC Cambridge Process in terms of separation of the metallic product from solidified molten salt in post-electrolysis processing. This finding also allows the use of some organic solvents that have a low but sufficient

solubility of the salts, but much lower reactivity to the as-produced metals, particularly rare earths [54].

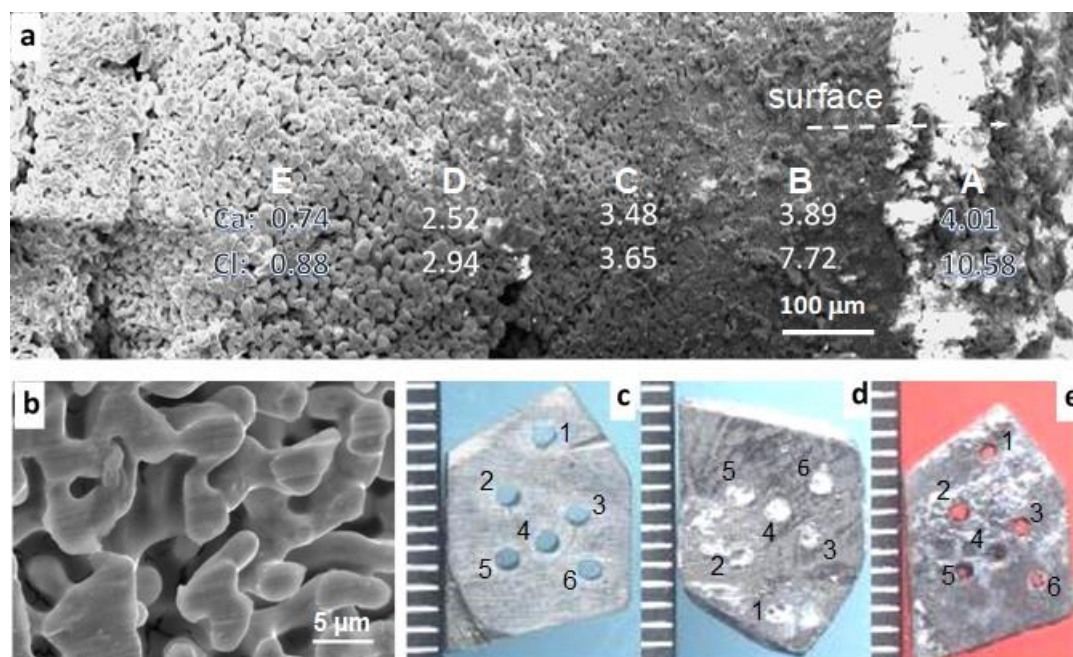


Figure 5. SEM images of (a) the cross section of a fully electro-reduced and unwashed porous pellet of Tb_2O_3 powder in molten $CaCl_2$ with EDX analysis results indicated for Ca, Cl and Tb (balancing), and (b) an enlarged view of Tb nodules in the fully electro-reduced Tb_2O_3 pellet with some being ground to reveal the non-porous cross section. Digital photographs of (c) a small piece of Tb foil with 6 drilled holes before, and (d) after immersion in molten $CaCl_2$ without electrolysis, showing all holes being filled with solidified salt, and (e) after electrolysis at 3.2 V for 30 min under argon, showing 5 of the 6 holes being free of solidified salt [53].

5. Carbon contamination

The use of a carbon anode is commonplace in molten salt electrolysis, and has been the case in most reported studies of the FFC Cambridge Process. Graphite is mostly used, although glassy carbon also helped a few fundamental studies. The advantages of using a graphite anode are basically commercial availability, shaping and processing convenience, thermal and chemical stability in molten salts, and good electronic conductivity. Obviously, according to

Reactions (2) and similar ones, emission of CO₂ from the FFC Cambridge Process using a carbon anode is inevitable. However, if cost of materials is correlated with CO₂ impact in the manufacturing stage, carbon anodes may still be a more acceptable choice in comparison with those inert anodes which are still under development. In fact, the more negative impact from using a carbon anode is carbon contamination on the cathodic products, which follows two mechanisms as explained below.

5.1. The carbonate cycling mechanism

It has been long recognised that in operation of the FFC Cambridge Process, the CO₂ gas produced on a carbon anode could be re-absorbed back into molten CaCl₂ and contaminate possibly the cathode product via Reactions (17) and (18) below [42,44,55].



It is worth noting that Reaction (18) was likely first reported in mid-1960 in molten carbonate salts [56,57], whilst later studies have suggested that this cathodic reaction could proceed in a wide range of molten salts as long as CO₃²⁻ and Li⁺ ions are present [18-21, 56-60].

Thermodynamic analyses of cathodic deposition of carbon and alkali or alkaline earth metals revealed that Ca²⁺ could also help cathodic deposition of carbon. This prediction was initially tested successfully in mixed CaCl₂ and CaCO₃ (84:16 in molar ratio) [60] but the applied temperature (730 °C) was higher than those of Li⁺ ion containing carbonates (<600 °C). The unique behaviour of Li⁺ and Ca²⁺ (and also Ba²⁺) ions may have resulted from their high affinity to the O²⁻ ion from Reaction (18) (or the molten salt). This affinity pushes the metal deposition potential negatively away from that for carbon deposition. The same does not apply to Na⁺ and K⁺ ions, leading to preference for metal deposition [60].

Unlike in molten carbonate salts or others with high CO₃²⁻ activities, Reaction (18) in molten chloride salts is highly likely diffusion controlled. Also, the fate of CO₃²⁻ in molten CaCl₂ will depend on the experimental conditions. Thermal decomposition of CaCO₃ occurs

at temperatures beyond 887 °C, which would reduce (but not likely eliminate) the CO_3^{2-} activity. At a sufficiently high activity, CO_3^{2-} may also compete with O^{2-} to discharge on the carbon anode according to Reaction (19) at a potential about 400 mV more positive than that of the reverse of Reaction (18) [60].



Therefore, largely depending on the O^{2-} activity in molten CaCl_2 , electro-reduction of TiO_2 does not necessarily always suffer from carbon contamination by Reaction (18).

A systematic study of the products from electro-reduction of TiO_2 precursors (cylindrical pellets) with different porosities revealed an interesting trend of carbon contamination in products from low porosity precursors, but not in those high porosity cases [61,62]. XRD patterns of these products are presented in Figure 6a. It should be noted that the XRD patterns of the electrolysed dense precursors were taken from the samples' surface materials because the cores were partially or not reduced. In another experiment, TiO_2 precursors of the same porosity (70%) were electrolysed in molten CaCl_2 with or without added CaO . The products were then analysed by XRD as shown in Figure 6b. In both cases, carbon contamination was represented by the detection of TiC in the electrolysis products. Considering findings from both experiments, it appears that the TiC phase formed disregarding the porosity of the TiO_2 precursors, but appeared in products from electrolysis for longer times. In addition, as expected, the XRD patterns in Figure 6b suggest convincingly a correlation of carbon contamination with the O^{2-} activity in the molten salt.

It was thought that the anodically generated CO_2 could travel to the cathode through both the gas and liquid phases. In the gas phase route, CO_2 entered the molten salt via Reaction (17) at the gas/liquid interface, particularly near the cathode. In the liquid path, the as-produced CO_2 immediately reacts with O^{2-} via Reaction (17) in the molten salt near the anode, and then transports to the cathode via convection and diffusion. Figure 7a illustrates schematically this understanding. In this mechanism, both time for mass transport of O^{2-} and CO_3^{2-} and O^{2-} activity for conversion of CO_2 to CO_3^{2-} play important roles.

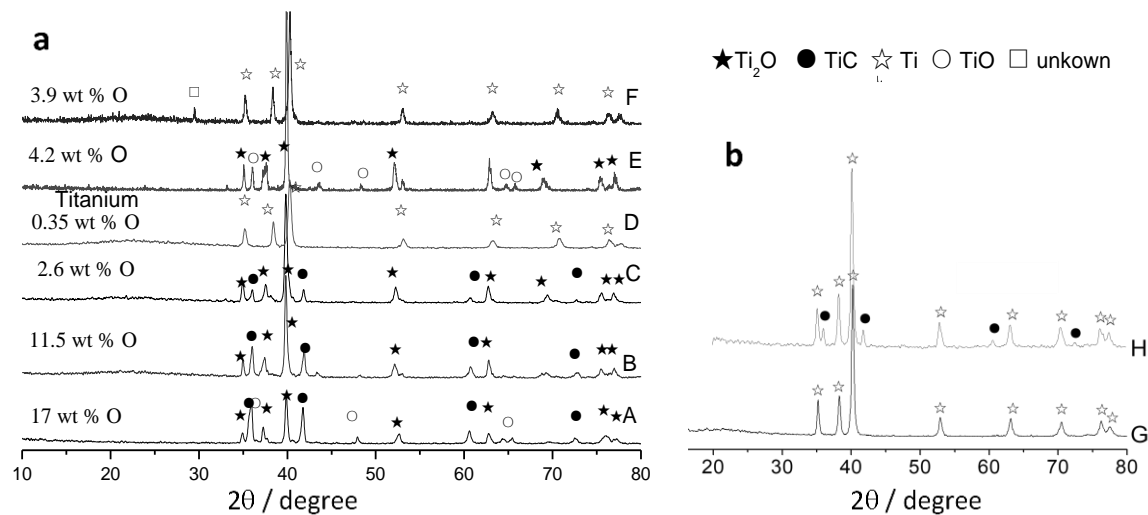


Figure 6. XRD patterns of products from electrolysis of (a) TiO_2 cylindrical pellets of different porosities (A: 12%, B: 23%, C: 44%, D: 68%, E: 77%, F: 80%) at 3.2 V in molten CaCl_2 for 5 hrs (A, B, C, surface materials) or 3 hrs (D, E, F, full body), and (b) TiO_2 pellets of 70% porosity in molten CaCl_2 at 3.0 V for 5 hrs (G), or in molten CaCl_2 + 5% CaO at 2.6 V for 11 hrs (H). Electrolysis temperature: 850 °C [61].

5.2. The carbon debris mechanism

The other mechanism for carbon contamination is unique to the quality of commercial graphite for making the anode. In laboratory studies of the FFC Cambridge Process, it is often observed a thin layer of carbon debris floating on the surface of the molten salt. Such debris could also, depending on sizes, suspend in, or precipitate to the bottom of the molten salt. In a scaling up test, a thick slug of carbon debris was seen on the top of molten CaCl_2 after electrolysis [63]. It is worth mentioning that various commercial graphite materials in the forms of rod and plate were used, but some of these performed better than the others in terms of stability, durability and contamination to the molten salt. Because graphite crucibles are commonly used to contain molten salts without contamination, it is believed that the observation of carbon debris was related to the anodic behaviour of graphite in CaCl_2 based molten salts.

This understanding agrees with experimental observations that graphite anodes were highly inert for discharging S^{2-} ions to the S_2 steam, or Cl^- ions to the Cl_2 gas in the molten mixtures of chloride salts with low O^{2-} solubility [33-36]. Specifically, carbon debris did not form in the molten mixture of $MgCl_2$, KCl and $NaCl$ which prevented O^{2-} ions from reaching the graphite anode by formation of insoluble MgO , and assisted successful electro-reduction of various metal oxides to the respective metals via anodic discharge of Cl^- ions to Cl_2 [36].

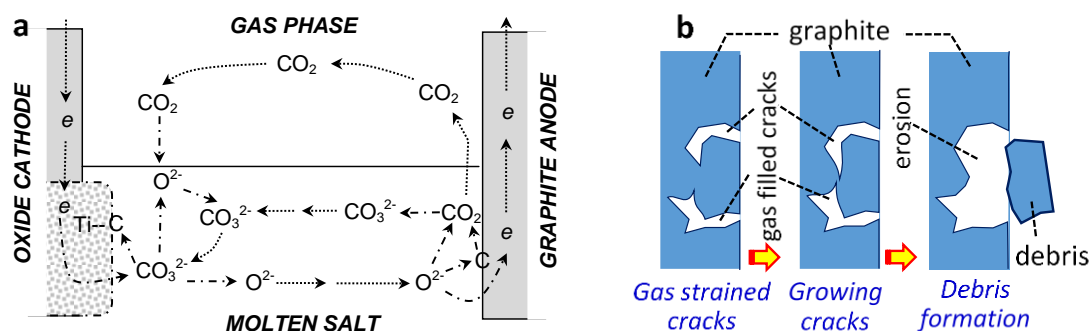


Figure 7. Schematic illustrations of two mechanisms of carbon transfer from the graphite anode to the oxide cathode during electrolysis of solid metal oxide (TiO_2) in molten salts. (a) Carbonate cycling mechanism: Chemical and cyclic conversion between cathodically discharged O^{2-} , anodically formed CO_2 , and chemically formed CO_3^{2-} that is electro-reduced to carbon and contaminates the cathode. (b) Carbon debris mechanism: Physical loss of carbon debris from the graphite anode by continuous formation of gas with an increasing pressure in cracks or pores that are either present originally in commercial graphite or formed by loss of carbon at anodically selected sites for CO or CO_2 formation, leading to eventual burst of the confined gas and formation of carbon debris that float on or suspend in the molten salt and eventually drift to contaminate the cathode [12].

Although there has not yet been a systematic study on the formation mechanisms of carbon debris, two reasonable assumptions are worth more discussion here. Firstly, the reduction of CO_3^{2-} , and likely directly CO_2 , to carbon can proceed at the

“gas/electrolyte/cathode current collector” three phase lines. Such produced carbon may detach from the cathode and float as debris on the molten salt surface. However, this cathodic carbon formation mechanism may have only played a secondary role in the formation of carbon debris, if any. This is because dedicated cathodic deposition of carbon in molten carbonates has very high current efficiency [18-20, 60], which means that most deposited carbon remained on the cathode upon collection.

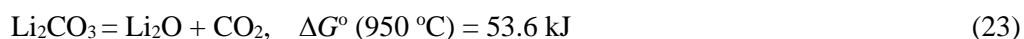
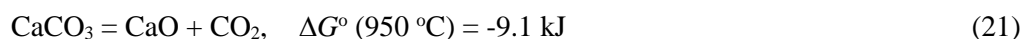
Secondly, it was commonly noticed that the graphite anode was not attacked or eroded uniformly after electrolysis, as shown in Figure 1h. In other words, the oxidative attack was selective. The theoretical density of graphite is 2.26 g/cm^3 whilst commercial graphite rods and plates are manufactured by densification of graphitic particles with densities commonly below 2.0 g/cm^3 . Thus, commercial graphite has always a certain level of porosity with the pores, voids or cracks existing more likely in the boundaries between the packed particles. Additional surface pores or cracks on the anode surface can result from oxidative attack by oxygen atoms and molecules formed from O^{2-} discharge, particularly to the boundaries. Such pores or cracks on the surface of a graphite anode would be filled with molten salt in which CO_2 forms. This process leads to two consequences. Firstly, the pore becomes deeper and wider due to carbon loss to CO_2 formation. Secondly, when the speed of CO_2 formation is faster than that for CO_2 to escape from the pore, pressure builds up in the pores. Eventually, the increased CO_2 gas pressure in the pores and the weakened connection between graphite particles jointly force the detachment of carbon debris into the molten salt. Figure 7b illustrates schematically this debris formation process on the carbon anode. Obviously, like the carbonate cycling mechanism, the carbon debris mechanism also takes time to proceed (to erode the anode gradually) and depends on the O^{2-} activity in the molten salt (to enable CO_2 formation in pores and cracks).

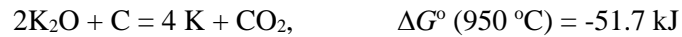
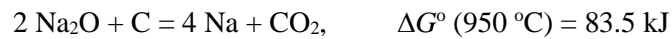
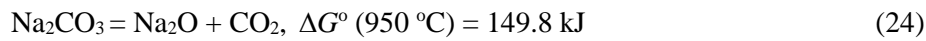
5.3. Prevention of carbon contamination

The above discussion indicates clearly that carbon contamination to the products in the FFC Cambridge Process originates from the use of a carbon anode. Therefore, as already discussed

above, the use of either an ionic blocking or conducting inert anode will eliminate this problem. Unfortunately, inert anodes are still under development, making graphite the more favoured choice in both laboratory and industry. Further, there are a few approaches that can help reduce the negative impact on the cathode from using a carbon anode. The followings discuss these approaches.

As mentioned above, the key step in the carbonate cycling mechanism is the reaction between CO_2 and O^{2-} in the molten salt near the anode, or at the gas/molten salt interface. However, decomposition of CaCO_3 to CaO and CO_2 occurs at temperatures above $887\text{ }^\circ\text{C}$. Thus, the carbonate cycling mechanism should be ineffective in molten CaCl_2 at higher electrolysis temperatures [23, 64]. Nevertheless, cautions should be applied when using this simple approach if the molten salts used contains other alkali and/or alkaline earth metal cations which can stabilise CO_3^{2-} against decomposition. As shown by Reactions (20) to (25), CaCO_3 decomposes, but Na_2CO_3 remains very stable, at $950\text{ }^\circ\text{C}$ [23]. Because CaCl_2 has been often mixed with other chloride salts to lower the liquidus temperature, the carbonate cycling mechanism would not change in such melts by raising the electrolysis temperatures. The following reactions also include those for electro-reduction of alkali or alkaline earth oxides against a carbon anode at $950\text{ }^\circ\text{C}$. In these cases, K_2O and Na_2O are much easier to electrolyse than the other oxides because Na and K are gases, whilst all the other listed alkali and alkaline earth metals are liquids at $950\text{ }^\circ\text{C}$ [23].





Therefore, to avoid carbon contamination via the carbonate cycling mechanism, it is recommended to operate the FFC Cambridge Process in pure CaCl_2 with the O^{2-} activity being as low as possible, but still at a sufficient level to maintain a good cathodic reaction rate and the anodic discharge of O^{2-} ions, instead of Cl^- ions. The working temperature should be above $900 \text{ }^\circ\text{C}$, but below $1000 \text{ }^\circ\text{C}$ to avoid serious salt evaporation.

Physically reducing the direct contact between carbon debris and the oxide cathode was attempted to mitigate carbon contamination from the cathode. An alumina tube (sheath) was used to enclose the oxide pellet cathode from the gas phase and block most mass movement between the anode and cathode in the molten salt, leaving only a small hole in the tube side wall to continue the ionic conduction path, as shown in Figure 8a [35,65,66]. This approach worked highly effectively in elimination of the effect of carbon debris.

Figure 8b and 8c compare the electrolysis products from the cell with and without using the alumina tube. Without using the tube, the as-electrolysed cathode was covered by solidified mixture of salt and carbon debris, whilst that electrolysed inside the tube showed clear solidified salt only. In addition, it was noticed that using the tube in the electrolysis led to a significantly lower current flow than that without using the tube, as shown in Figure 8d, but the oxide pellet that was electro-reduced inside the tube could reach an oxygen content about 15% lower than that without using the tube [65]. These findings are indication of higher current and energy efficiencies. The efficiency derived from the electrolysis data in Figure 8d was almost twice improved by using the alumina tube [66].

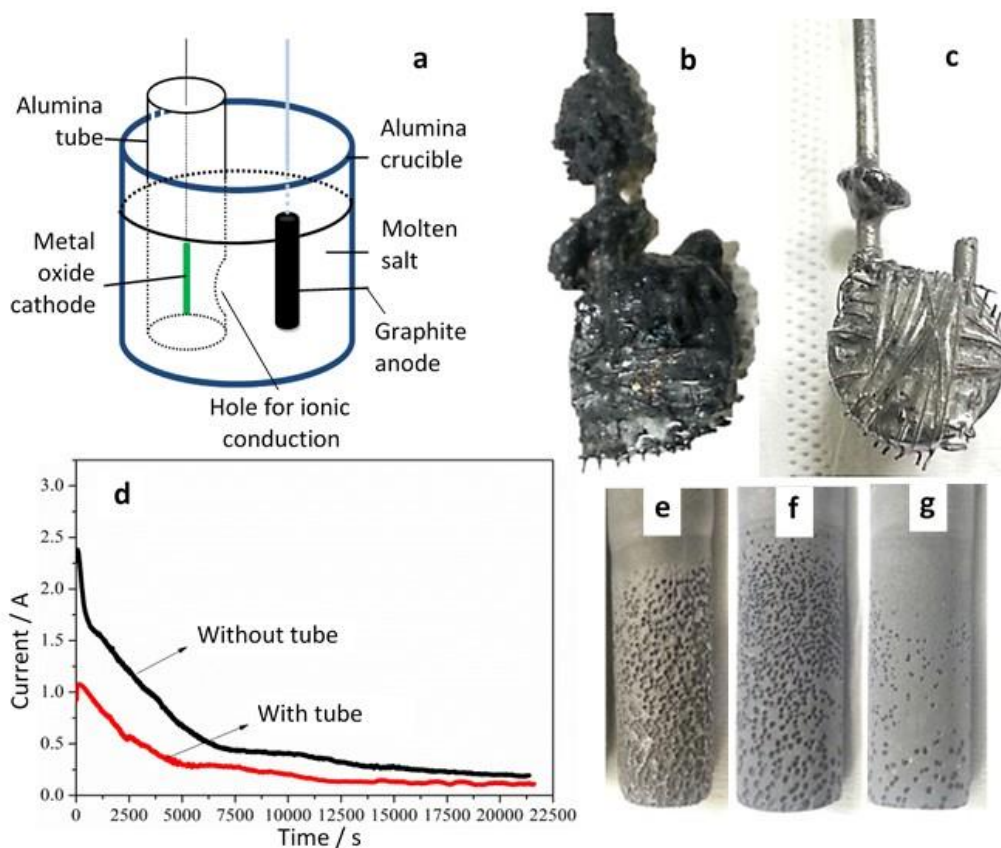


Figure 8. (a) Schematic diagram of a modified FFC cell with a graphite rod anode and an oxide pellet cathode (1 g Cr_2O_3 wrapped by Mo wire) that is sheathed in an alumina tube whose internal and external molten salts are connected via a small hole on the alumina tube side wall facing the graphite anode. (b, c) Photographs of electrolysed oxide cathodes without (b) and with (c) using the alumina sheath. (d) Current-time curves of electrolysis of Cr_2O_3 pellets at 2.80 V and 810 °C without and with using the sheathing alumina tube. (e - g) Photographs of graphite anodes after electrolysis of Cr_2O_3 pellets without (e) and with using the alumina tube (f: frontside that was facing the hole during electrolysis; g: backside) [65,66].

Such a significant improvement had obviously benefited from the sheathing tube not only blocking electronic conduction through the floating carbon debris, but also reducing the carbonate cycling. Whilst CO_2 transfer via the gas phase near the cathode was completely blocked, the route for CO_3^{2-} cycling through the molten salt was also significantly narrowed

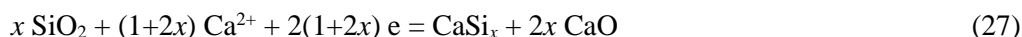
by the small hole in the tube sidewall. The consequence would be that most CO_3^{2-} ions, if not all, in the molten salt were unable to reach the cathode in the same time interval, but remained in molten salt outside the sheathing tube. This in turn reduced the amount of O^{2-} ions produced by Reaction (18), and hence the O^{2-} activity and flux in the molten salt. This understanding was supported by the obvious difference in anode erosion represented by the photographs in Figure 8e, and 8f and 8g.

Without using the sheathing tube, the graphite anode suffered serious erosion and thinning, see Figure 8e which is similar to that in Figure 1h, but much less erosion occurred to the graphite anode, shown in Figures 8f and 8g, that was coupled with the alumina tube sheathed cathode. It is interesting to note that erosion occurred around the graphite anode in absence of the sheathing tube, but it was more notable in the frontside facing the hole of the tube than on the backside, as shown in Figure 8f and 8g, respectively. These are strong evidence that the O^{2-} flux was smaller from the tube sheathed cathode, than that from the naked cathode, to the graphite anode, which can be explained by reduced CO_3^{2-} cycling. Also, because the discharge of the O^{2-} is driven by the electric field in the interfacial layer between the electrode and electrolyte, i.e. the electric double layer, the difference between Figure 8f and 8g is indicative of difference in the electric field strength. This was less likely caused by the potential distribution around the graphite anode which is a good electronic conductor. It can be attributed to the greater O^{2-} activity and flux in front of the anode facing the hole of the sheathing tube. It is expected that if the anode was placed sufficiently distant away from the hole of the tube, the frontside and backside of the anode would have behaved more similarly as diffusion and convection should even out the O^{2-} distribution around the anode.

6. Other interactions

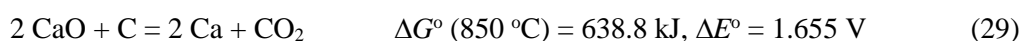
The above discussed three main interactions are common to all metal oxides to be reduced in the FFC Cambridge Process. However, some interactions are specific to the metal oxides, or the metals produced. For example, SiO_2 can be electro-reduced in molten CaCl_2 to Si which can react with Ca or Ca^{2+} at appropriate cathodic potentials to form various calcium silicides,

CaSi_x with *x* varying between 0.5 and 2.0 [67-69]. Reactions (26) and (27) below represent the chemical and electrochemical formation of CaSi_x, in which Ca may be assumed to result from the electro-reduction of Ca²⁺ ions under some depolarisation conditions, e.g. on the surface of Si, although the actual origin of Ca is thermodynamically irrelevant.



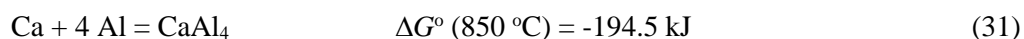
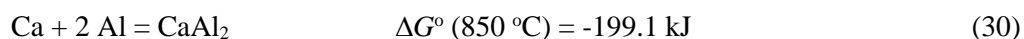
Because formation of CaSi_x occurs at potentials more positive than that for Ca deposition, the potential window for electro-reduction of SiO₂ to pure Si is very much limited [67]. Whilst a robust reference electrode [70-72] could help perform constant potential electrolysis in laboratory to avoid CaSi_x formation, its application can be a great challenge in an industrial cell. The use of a computer-aided control (CAC) of the cell voltage programme may offer a promising direction in industrial production [45]. This approach is simple, energy saving and low cost. The principle of CAC is basically to programme the cell voltage - time profile following that recorded in a successful test of constant potential electrolysis.

Aluminium (Al) is difficult to produce from its oxide, Al₂O₃, in the FFC Cambridge Process, although thermodynamics could predict clear feasibility as shown by Reactions (28) and (29).



The difficulty is partly because the melting point ($\approx 660.3 \text{ }^\circ\text{C}$) of Al is too low and liquid Al does not dissolve oxygen. More importantly the reduction potential of Al₂O₃ is only 0.40 V more positive than that for Ca deposition. Such a small difference can be easily overtaken by the polarisation needed to reduce the very insulating Al₂O₃, which means the produced Al will react with Ca readily to form aluminides (CaAl_x, *x* = 2, 4). Also, similar to the case of Ca deposition on Si, deposition of Ca on liquid Al could be more depolarised and effective to

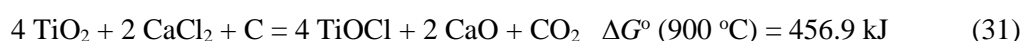
form CaAl_x . The positive shift of the potential for Ca deposition on Al via Reactions (30) and (31) could be 1.032 V and 1.008 V, respectively, which are greater than the difference between Reactions (28) and (29).



The literature is lack of sufficient research on electro-reduction of solid Al_2O_3 , although one report claimed successful production of pure Al [73], but the other described both thermodynamic and experimental findings of formation of CaAl_x [74]. A more recent study found that when the Al_2O_3 powder was used on the cathode, electroreduction produced CaAl_2 , whilst pure Al beads were collected from potentiostatic electrolysis of dense alumina (e.g. a small section of Al_2O_3 tube). It was thought that electrolysis of the small Al_2O_3 tube was favourable for the O^{2-} ion to diffuse away from the reaction site, i.e. the Al/ Al_2O_3 /electrolyte 3PIs, leaving behind a sufficiently low O^{2-} activity (high $p\text{O}^{2-}$ value) that helped production of pure Al as predicted by thermodynamic analysis [75]. However, when electro-reducing the Al_2O_3 powder, diffusion in the pores between powder particles was too slow, leading to higher O^{2-} activities to encourage formation, in analogy to perovskitisation, of various calcium aluminates between $\text{Ca}_3\text{Al}_2\text{O}_6$ and $\text{CaAl}_{12}\text{O}_{19}$ ($x\text{CaO} \cdot y\text{Al}_2\text{O}_3$, $x = 1$ to 3 ; $y = 1$ to 6) whose electro-reduction could only produce CaAl_x . Obviously, the application of a constant cathodic potential was the key for the improved electrolysis result. It is worth pointing out that current industrial production of pure Al is achieved at large scale by electrolysis of dissolved Al_2O_3 in molten fluoride salts with high rate and high efficiency. Therefore, direct electro-reduction of solid Al_2O_3 to Al in molten chloride salts remains a fundamental interest.

As it has been discussed above, research on the FFC Cambridge Process in the past 20 years has been successful in making targeted metallic products, thanks to the relatively high stability of the relevant metal oxides and sulfides in CaCl_2 (or LiCl) based molten salts. However, it was also found that formation of oxychlorides could occur during electro-

reduction of metal oxides to different extents. The awareness of oxychloride formation came from an early observation of yellowish condensate [76] on the surface of the upper portions of a long graphite anode for electrolysis of TiO₂ in molten CaCl₂, see Figure 1f. EDX analysis of the condensate indicated presence of Ti, O and Cl together with CaCl₂, which agrees with Reaction (31). Note that the Ti valence in TiOCl is III, suggesting the reaction having occurred upon partial reduction of the TiO₂ cathode. It is fortunate that Reaction (31) is only a side reaction, accounting for an insignificant percentage of the TiO₂ feed.



Most literatures on electro-reduction of metal oxides have not focused on formation of oxychloride which however could occur between most rare earth (Re) metal oxides and molten CaCl₂. Specially, lanthanum oxide (La₂O₃) reacts spontaneously with molten CaCl₂ to produce LaOCl which may dissolve, at least partly, in CaCl₂.

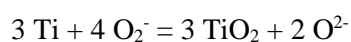
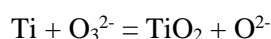


Therefore, it is out of question to use molten CaCl₂ for electro-reduction of La₂O₃, but it may still be feasible in molten LiCl. Nevertheless, it was shown that the oxychloride issue could be avoided effectively by pre-compounding La₂O₃ with NiO [77]. In doing so, various AB₅ hydrogen storage alloys (HSAs) such as LaNi₅ and LaNi₄Co were prepared successfully by electroreduction in molten CaCl₂ at high yields with the energy consumption being as low as 4.54 kWh/kg-LaNi₅. After washing in water or DMSO, the as-produced HSAs all showed good charging-discharging performances. The obtained LaNi₄Co powder performed most satisfactorily. A maximum discharging capacity of 325 mAh/g was recorded, which is close to the theoretical capacity of 371.9 mAh/g for LaNi₅ + 3 H₂ = LaNi₅H₂.

Last, but not the least, in the FFC Cambridge Process, air-isolated high temperature molten salts (e.g. CaCl₂, LiCl and their mixtures with other salts) are used as the electrolyte. The applied high temperature helps lower the kinetic barriers for electrochemical reduction of semiconducting and insulating solid metal oxides or sulfides to the respective metals. Air

isolation, together with inert gas purging, is the most essential key to the success of the FFC Cambridge Process. To achieve air-isolation, it is crucial that the molten salt electrolyser is strictly sealed in a reaction vessel. There has been a general thought that because argon (Ar) is heavier than air, it can sink in the vessel and protect the electrolyser and cathode product from oxidation by the oxygen in air. This is an unfortunate misunderstanding and needs clarification. It can be derived from the Gibbs energy changes of Reactions (1) and (8) that the equilibrium partial pressures of oxygen are 2.50×10^{-33} atm and 4.60×10^{-39} atm, respectively, whilst the oxygen partial pressure in air is 0.21 atm. This ultra large difference in oxygen partial pressure means a huge rate for oxygen to diffuse from air into the reaction vessel, even just through small a leaking gap.

Another misunderstanding is that the molten salt may provide a physical barrier for direct contact between the cathode product and air, and hence protecting the former from oxidation. The truth is that when O^{2-} ions are present in a $CaCl_2$ or $LiCl$ based melt, which is inevitable in the FFC Cambridge Process, they could function as a phase transfer catalyst and transfer oxygen from the gas phase to the metal on cathode in the molten salt by formation of peroxide (O_3^{2-}) and superoxide (O_2^-) anions via Reactions (34) and (35) below [78].



It can be seen from these two reactions that the O^{2-} ion transfers oxygen, as a vehicle offering the return service, from the gas phase to the Ti metal on cathode in the molten salt. After reaction with the metal, the O^{2-} ion is released back to the melt to bring more oxygen into the melt. Therefore, these two factors will together make it impossible to electro-reduce a metal oxide to the metal with a sufficiently low oxygen content.

7. Summary

The FFC Cambridge Process has been in research and development for over two decades, embracing various successes but also challenges. Three generic interactions between the cathode product and molten salt, specifically CaCl_2 , have been identified as (1) perovskitisation and similar reactions that include Ca into the cathode without oxygen removal, (2) non-wetting of molten salts on pure metal surfaces, which helps separation of solidified salt in the final product, and (3) carbon contamination via either or both of the carbonate cycling and carbon debris mechanisms. In addition, observation and the mechanisms of formation of calcium silicides and calcium aluminides, formation of oxychlorides, and the problem of an unsealed or leaky reaction vessel are also discussed briefly. In all discussed cases of interactions, it is shown that proper understanding of the causes and mechanisms of these interactions are the key to development and experimental demonstration of feasible approaches to the desirable solutions.

In addition to what has been discussed on using more porous oxide precursor to speed up electro-reduction, it is worth mentioning that a few studies were carried out on oxide pellets of very low porosity ($\leq 30\%$), capturing more details of intermediate phases [79-81]. Another uncovered area of interest and technological importance is nuclear fuel processing [82,83], which deserves a separate specialist analysis. Further, the literature of the past two decades has included numerous comprehensive or specific topic review articles on the FFC Cambridge Process, all showing positive and encouraging views on the prospects [6-12,40,50,69,84-86]. What has also emerged in the literature is the scaling-up studies of the FFC Cambridge Process with promising results for eventual commercialisation [13,14,85-87].

8. Acknowledgement

(See the title page)

9. References

- [1] D.J. Fray, T.W. Farthing, and Z. Chen, *Removal of oxygen from metal oxides and solid solutions by electrolysis in a fused salt*, Int. Patent, WO9964638, 1999.
- [2] G.Z. Chen, D.J. Fray, and T.W. Farthing, Direct electrochemical reduction of titanium dioxide to titanium in molten calcium chloride, *Nature*, 407(2000), p. 361.
- [3] H.M. Flower, A moving oxygen story, *Nature*, 407(2000), p. 305.
- [4] Science and Technology, Dr. Chen and the philosopher's stone, *The Economist*, 21st September 2000. <https://www.economist.com/science-and-technology/2000/09/21/dr-chen-and-the-philosophers-stone> (accessed on 04 May 2020)
- [5] K. Faller and F.H.S. Froes, The use of titanium in family automobiles: Current trends, *JOM*, 53(2001), p.27.
- [6] D.J. Fray and G.Z. Chen, Reduction of metal oxides using electro-deoxidation, *Mater. Sci. Tech.*, 20(2004), p.295.
- [7] G.Z. Chen and D.J. Fray, Understanding the electro-reduction of metal oxides in molten salts, *Light Metals 2004*, (2004), p. 881.
- [8] D.H. Wang, X.B. Jin, and G.Z. Chen, Solid state reactions: An electrochemical approach in molten salts, *Annu. Rep. Prog. Chem., Sect. C: Phys. Chem.*, 104(2008), p. 189.
- [9] W. Xiao and D.H. Wang, The electrochemical reduction processes of solid compounds in high temperature molten salts, *Chem. Soc. Rev.*, 43(2014), p. 3215.
- [10] D.J. Fray and C. Schwandt, Aspects of the application of electrochemistry to the extraction of titanium and its applications, *Mater. Trans.*, 58(2017), p. 306.
- [11] D. Hu and G.Z. Chen, Chapter 25 - Advanced extractive electrometallurgy, [in] Breitkopf C, Swider-Lyons K, eds., *Springer Handbook of Electrochemical Energy*, Springer, London, 2017, p. 801.
- [12] G.Z. Chen and D.J. Fray, Chapter 11 - Invention and fundamentals of the FFC Cambridge Process, [in] Fang ZZ, Froes HS, Zhang Y, eds., *Extractive Metallurgy of Titanium - Conventional and Recent Advances in Extraction and Production of Titanium Metal*, Elsevier, Oxford, 2020, p. 227

- [13] Metalysis, Technology, 2019. <http://www.metalysis.com/technology/>.
- [14] GLABAT, Development of Negative Electrode Materials, 2015. <http://www.glabat.com/article/content/view?id=23>.
- [15] D. Hu, W. Xiao, and G.Z. Chen, Near-net-shape production of hollow titanium alloy components via electrochemical reduction of metal oxide precursors in molten salts, *Metall. Mater. Trans. B*, 44(2013), p. 272.
- [16] C. Schwandt, J.A. Hamilton, D.J. Fray, and I.A. Crawford, The production of oxygen and metal from lunar regolith, *Planetary Space Sci.*, 74(2012), p. 49.
- [17] B.A. Lomax, M. Conti, N. Khan, N.S. Bennett, A.Y. Ganin, and M.S. Symes, Proving the viability of an electrochemical process for the simultaneous extraction of oxygen and production of metal alloys from lunar regolith, *Planetary Space Sci.*, 180(2020), art. No. 104748.
- [18] N.J. Siambun, H. Mohamed, D. Hu, D. Jewell, Y.K. Beng, and G.Z. Chen, Utilisation of carbon dioxide for electro-carburisation of mild steel in molten carbonate salts, *J. Electrochem. Soc.*, 158(2011), p. H1117.
- [19] D. Tang, H. Yin, X. Mao, W. Xiao, D.H. Wang, Effects of applied voltage and temperature on the electrochemical production of carbon powders from CO₂ in molten salt with an inert anode. *Electrochim. Acta*, 114(2013), p. 567.
- [20] W. Wang, B. Jiang, Z. Wang, and W. Xiao, In situ electrochemical conversion of CO₂ in molten salts to advanced energy materials with reduced carbon emissions, *Sci. Adv.*, 6(2020) eaay9278.
- [21] O. Al-Juboori, F. Sher, A. Hazafa, M.K. Khan, and G.Z. Chen, The effect of variable operating parameters for hydrocarbon fuel formation from CO₂ by molten salts electrolysis, *J. CO₂ Util.*, 40(2020), art. No.101193.
- [22] C. Peng, C.Z. Guan, J. Lin, S.Y. Zhang, H.L. Bao, Y. Wang, G.O. Xiao, G.Z. Chen, and J.Q. Wang, A rechargeable high-temperature molten salt iron-oxygen battery, *ChemSusChem*, 11(2018), p. 1880.
- [23] Outotec. *HSC Chemistry 2012*, 7.

- [24] H.L. Chen, X.B. Jin, L.P. Yu, and G.Z. Chen, Influences of graphite anode area on electrolysis of solid metal oxides in molten salts, *J. Solid State Electrochem.*, 18(2014), p. 3317.
- [25] G.Z. Chen and D.J. Fray, Cathodic refining in molten salts: Removal of oxygen, sulfur and selenium from static and flowing molten copper, *J. Appl. Electrochem.*, 31(2001), p. 155.
- [26] M. Mohamedi, B. Borresen, G.M. Haarberg, and R. Tunold, Anodic behavior of carbon electrodes in CaO - CaCl₂ melts at 1123 K, *J. Electrochem. Soc.*, 146(1999), p. 1472.
- [27] G.Z. Chen and D.J. Fray, Voltammetric studies of the oxygen-titanium binary system in molten calcium chloride, *J. Electrochem. Soc.*, 149(2002), p. E455.
- [28] R. Barnett, K.T. Kilby, and D.J. Fray, Reduction of tantalum pentoxide using graphite and tin-oxide-based anodes via the FFC-Cambridge Process, *Metall. Mater. Trans. B*, 40(2009), p. 150.
- [29] L.W. Hu, Y. Song, J.B. Ge, S.Q. Jiao, and J. Cheng, Electrochemical metallurgy in CaCl₂-CaO melts on the basis of TiO₂·RuO₂ inert anode, *J. Electrochem. Soc.*, 163(2016), p. E33.
- [30] T.A. Ramanarayanan and R.A. Rapp, The diffusivity and solubility of oxygen in liquid tin and solid silver and the diffusivity, *Metall. Trans.*, 3(1972), p3239.
- [31] X.L. Zou, X.G. Lu, Z.F. Zhou, and C.H. Li, Direct electrosynthesis of Ti₅Si₃/TiC composites from their oxides/C precursors in molten calcium chloride, *Electrochem. Commun.*, 21(2012), p. 9.
- [32] H.B. Hu, Y.M. Gao, Y.G. Lao, Q.W. Qin, G.Q. Li, and G.Z. Chen, Yttria stabilized zirconia aided electrochemical investigation on ferric ions in mixed molten calcium and sodium chlorides, *Mater. Metall. Trans. B*, 49(2018), p. 2794.
- [33] T. Wang, H.P. Gao, X.B. Jin, H.L. Chen, J.J. Peng, and G.Z. Chen, Electrolysis of solid metal sulfide to metal and sulfur in molten NaCl-KCl, *Electrochem. Commun.*, 13(2011), p. 1492.

- [34] C.H. Wu, M.S. Tan, G.Z. Ye, D.J. Fray, and X.B. Jin, High-efficiency preparation of titanium through electrolysis of carbo-sulfurized titanium dioxide, *ACS Sust Chem Eng*, 7(2019), p. 8340.
- [35] W. Li, Y.T. Yuan, X.B. Jin, H.L. Chen, and G.Z. Chen, Environmental and energy gains from using molten magnesium–sodium–potassium chlorides for electro-metallisation of refractory metal oxides, *Prog. Nat. Sci. Mater. Int.*, (Sp. Iss) 25(2015), p. 650.
- [36] Y.T. Yuan, W. Li, H.L. Chen, Z.Y. Wang, X.B. Jin, and G.Z. Chen, Electrolysis of metal oxides in MgCl₂ based molten salts with an inert graphite anode, *Faraday Discuss.*, 190(2016), p. 85.
- [37] D. Sadoway, Inert anodes for the Hall-Heroult cell: The ultimate materials challenge, *JOM*, 53(2001), p. 34.
- [38] H.Y. Yin, L.L. Gao, H. Zhu, X.H. Mao, F.X. Gan, and D.H. Wang, On the development of metallic inert anode for molten CaCl₂–CaO system, *Electrochim. Acta*, 56(2011), p. 3296.
- [39] H.Y. Yin, D.Y. Tang, H. Zhu, Y. Zhang, and D.H. Wang, Production of iron and oxygen in molten K₂CO₃-Na₂CO₃ by electrochemically splitting Fe₂O₃ using a cost affordable inert anode, *Electrochem. Commun.*, 13(2011), p. 1521.
- [40] D.H. Wang and W. Xiao, Chapter 9 - Inert anode development for high-temperature molten salts, [in] F. Lantelme, H. Groult, eds., *Molten Salts Chemistry - From Lab to Applications*, Elsevier, Oxford, 2013, p. 171.
- [41] C. Schwandt and D. J. Fray, Use of molten salt fluxes and cathodic protection for preventing the oxidation of titanium at elevated temperatures, *Metall. Mater. Trans. B*, 45(2014), p. 2145.
- [42] C. Schwandt and D.J. Fray, Determination of the kinetic pathway in the electrochemical reduction of titanium dioxide in molten calcium chloride, *Electrochim. Acta*, 51(2005), p. 66.
- [43] K. Jiang, X.H. Hu, M. Ma, D.H. Wang, G.H. Qiu, X.B. Jin, and G.Z. Chen, Perovskitization assisted electrochemical reduction of solid TiO₂ in molten CaCl₂, *Angew. Chem. Int. Ed.*, 45(2006), p. 428.

- [44] E. Gordo, G.Z. Chen, and D.J. Fray, Toward optimisation of electrolytic reduction of solid chromium oxide to chromium powder in molten chloride salts, *Electrochim. Acta*, 49(2004), p. 2195.
- [45] T. Wu, X.B. Jin, W. Xiao, C. Liu, D.H. Wang, and G.Z. Chen, Computer-aided control of electrolysis of solid Nb₂O₅ in molten CaCl₂, *Phys. Chem. Chem. Phys.*, 10(2008), p. 1809.
- [46] G.Z. Chen, E. Gordo, and D.J. Fray, Direct electrolytic preparation of chromium powder, *Metall. Mater. Trans. B*, 35(2004), p. 223.
- [47] Y. Deng, D.H. Wang, W. Xiao, X.B. Jin, X.H. Hu, and G.Z. Chen, Electrochemistry at conductor / insulator / electrolyte three-phase interlines: A thin layer model, *J. Phys. Chem. B*, 109(2005), p. 14043.
- [48] W. Xiao, X.B. Jin, Y. Deng, D.H. Wang, and G.Z. Chen, Three-phase interlines electrochemically driven into insulator compounds: A penetration model and its verification by electroreduction of solid AgCl, *Chem. Eur. J.*, 13(2007), p. 604.
- [49] W. Li, X.B. Jin, F.L. Huang, and G.Z. Chen, Metal-to-oxide molar volume ratio: The overlooked barrier to solid-state electro-reduction and a green bypass through recyclable NH₄HCO₃, *Angew. Chem. Int. Edit.*, 49(2010), p. 3203.
- [50] G.Z. Chen and D.J. Fray, A morphological study of the FFC chromium and titanium powders, *Mineral Processing and Extractive Metallurgy, (Trans. Inst. Min. Metall. Sect. C)* 115(2006), p. 49.
- [51] TWI Ltd. What is friction welding? <https://www.twi-global.com/technical-knowledge/faqs/faq-what-is-friction-welding> (accessed on 04 July 2020)
- [52] A.J. Muir Wood, R.C. Copcutt, G.Z. Chen, and D.J. Fray, Electrochemical fabrication of nickel manganese gallium alloy powder, *Adv. Eng. Mater.*, 5(2003), p. 650.
- [53] D.H. Wang, G.H. Qiu, X.B. Jin, X.H. Hu, and G.Z. Chen, Electrochemical metallisation of solid terbium oxide, *Angew. Chem. Int. Edit.*, 45(2006), p. 2384.
- [54] G.H. Qiu, D.H. Wang, M. Ma, X.B. Jin, and G.Z. Chen, Electrolytic Synthesis of TbFe₂ from Tb₄O₇ and Fe₂O₃ Powders in Molten CaCl₂, *J. Electroanal. Chem.*, 589(2006), p. 139.

- [55] P.C. Pistorius and D.J. Fray, Formation of silicon by electrodeoxidation, and implications for titanium metal production, *J. South African Inst. Mining Metall.*, 106(2006) p. 31.
- [56] Y.K. Delimarskii, O.V. Gorodiskii, and V.F. Grishchenko, Cathode liberation of carbon from molten carbonates, *Dokl. Akad. Nauk SSSR*, 156(1964), p. 650.
- [57] M. D. Ingram, B. Baron, and G. J. Janz, The electrolytic deposition of carbon from fused carbonates, *Electrochim. Acta*, 11(1966), p. 1629.
- [58] H. Kawamura and Y. Ito, Electrodeposition of cohesive carbon films on aluminum in a LiCl–KCl–K₂CO₃ melt, *J. Appl. Electrochem.*, 30(2000), p. 571.
- [59] L. Massot, P. Chamelot, F. Bouyer, and P. Taxil, Studies of carbon nucleation phenomena in molten alkaline fluoride media, *Electrochim. Acta*, 48,(2003), p. 465.
- [60] H.V. Ijije, R.C. Lawrence, N.J. Siambun, S. Jeong, D.A. Jewell, D. Hu, and G.Z. Chen, Electro-deposition and re-oxidation of carbon in carbonate containing molten salts, *Farad. Discuss.*, 172(2014), p. 105.
- [61] W. Li, H.L. Chen, F.L. Huang, X.B. Jin, F.M. Xiao, and G.Z. Chen, Fast electro-reduction of TiO₂ precursors with macro-micro-bimodal porosity in molten CaCl₂, *The 3rd Asia Conference on Molten Salts and Ionic Liquids*, 06-09 Jan. 2011, Harbin, P. R. China.
- [62] W. Li, Studies of new mode and mechanism for electrolysis of solid oxides in molten salts, *PhD Thesis*, Wuhan University, May 2010.
- [63] K. Dring, Direct electrochemical production of titanium, *3rd Reactive Metals Workshop*, 2-3, March, 2007, MIT, Cambridge, USA. http://www.okabe.iis.u-tokyo.ac.jp/core-to-core/rmw/RMW3/slide/RMW3_06_Dring_F.pdf [accessed on 09.07.2020].
- [64] G.Z. Chen and D.J. Fray, *Prevention of unwanted reactions at three phase boundaries*, UK Patent, Appl. GB0329541.7, 2003.
- [65] A. Stevenson, D. Hu, M.L. Hu, and G.Z. Chen, *Unpublished Results*, University of Nottingham, August 2013 to August 2014

- [66] M.L. Hu, Q. Zhengfeng, B. Chenguang, D. Hu, and G.Z. Chen, Effect of the changed electrolytic cell on the current efficiency in FFC Cambridge Process, *Mater. Trans.*, 58(2017), p. 322.
- [67] W. Xiao, X.B. Jin, Y. Deng, D.H. Wang, and G.Z. Chen, Rationalisation and optimisation of solid state electro-reduction of SiO₂ to Si in molten CaCl₂ in accordance with dynamic three phase interlines based voltammetry, *J. Electroanal. Chem.*, 639(2010), p. 130.
- [68] X. Yang, K. Yasuda, T. Nohira, R. Hagiwara, and T. Homma. Cathodic potential dependence of electrochemical reduction of SiO₂ granules in molten CaCl₂, *Metall. Mater. Trans. E*, 3(2016), p. 145.
- [69] E. Juzeliunas and D.J. Fray, Silicon electrochemistry in molten salts, *Chem. Rev.*, 120(2020), p. 1690.
- [70] P. Gao, X.B. Jin, D.H. Wang, X.H. Hu, and G.Z. Chen, A quartz sealed Ag/AgCl reference electrode for CaCl₂ based molten salts, *J. Electroanal. Chem.*, 579(2005), p. 321.
- [71] H. Wang, N.J. Siambun, L.P. Yu, and G.Z. Chen, A robust alumina membrane reference electrode for high temperature molten salts, *J. Electrochem. Soc.*, 159(2012), p. H740.
- [72] N.K. Al-Shara, F. Sher, A. Yaqoob, and G.Z. Chen, Electrochemical investigation of novel reference electrode Ni/Ni(OH)₂ in comparison with silver and platinum inert quasi-reference electrodes for electrolysis in eutectic molten hydroxide, *Int. J. Hydrogen Energy*, 44(2020), p. 27224.
- [73] H.W. Xie, H. Zhang, Y.H. Zhai, J.X. Wang, and C.D. Li, Al Preparation from Solid Al₂O₃ by direct electrochemical deoxidation in molten CaCl₂-NaCl at 550°C, *J. Mater. Sci. Technol.*, 25(2009), p. 459.
- [74] X.Y. Yan, and D.J. Fray, Direct electrolytic reduction of solid alumina using molten calcium chloride-alkali chloride electrolytes, *J. App. Electrochem.*, 39(2009), p. 1349.
- [75] H. Kadowaki, Y. Katasho, K. Yasuda, and T. Nohira, Electrolytic Reduction of Solid Al₂O₃ to Liquid Al in Molten CaCl₂, *J. Electrochem. Soc.*, 165(2018), p. D83.
- [76] R.J.H. Clark, D.C. Bradley, and P. Thornton, *The Chemistry of Titanium, Zirconium and Hafnium*, Pergamon Press, Oxford, 1973, p. 367.

- [77] Y. Zhu, D.H. Wang, M. Ma, X.H. Hu, X.B. Jin, and G.Z. Chen, More affordable electrolytic LaNi₅-type hydrogen storage powders, *Chem. Commun.*, (2007), p. 2515.
- [78] G.Z. Chen, D.J. Fray, and T.W. Farthing, Cathodic deoxygenation of the alpha-case on titanium and alloys in molten calcium chloride, *Metall. Mater. Trans. B*, 32(2001) , p.1041.
- [79] D.J. Fray, Novel methods for the production of titanium, *Int. Mater. Rev.*, 53(2008), p. 317.
- [80] D.T.L. Alexander, C. Schwandt, and D.J. Fray, Microstructural kinetics of phase transformations during electrochemical reduction of titanium dioxide in molten calcium chloride, *Acta Mater.*, 54(2006), p. 2933.
- [81] D. Sri Maha Vishnu, N. Sanil, L. Shakila, G. Panneerselvam, R. Sudha, K.S. Mohandas, and K. Nagarajan, A study of the reaction pathways during electrochemical reduction of dense Nb₂O₅ pellets in molten CaCl₂ medium, *Electrochim. Acta*, 100(2013), p. 51.
- [82] E.-Y. Choi, J.W. Lee, J.J. Park, J.-M. Hur, J.-K. Kim, K. Y. Jung, and S.M. Jeong, Electrochemical reduction behavior of a highly porous SIMFUEL particle in a LiCl molten salt, *Chem. Eng. J.* 207-208(2012), p. 514.
- [83] A. Stevenson, D. Hu, and G.Z. Chen, Molten salt assisted electrochemical separation of spent fuel surrogates by partial direct reduction and selective anodic dissolution, *ECS Trans.*, 64(2014), p.333.
- [84] K.S. Mohandas, Direct electrochemical conversion of metal oxides to metal by molten salt electrolysis: A review, *Miner. Process. Extract. Metall.*, 122(2013), p. 195.
- [85] C. Schwandt, G.R. Doughty, and D.J. Fray, The FFC-Cambridge Process for titanium metal winning, *Key Eng. Mater.*, 436(2010), p. 13.
- [86] D. Hu, A. Dolganov, M.C. Ma, B. Bhattacharya, M. Bishop, and G.Z. Chen, Development of the Fray-Farthing-Chen Cambridge Process: Towards the sustainable production of titanium and its alloys, *JOM*, 70(2018), p. 129.

[87] Z.L. Yu, N. Wang, S. Fang, X.P. Qi, Z.F. Gao, J.Y. Yang, and S.G. Lu, Pilot-plant production of high-performance silicon nanowires by molten salt electrolysis of silica, *Ind. Eng. Chem. Res.*, 59(2020), p. 1.